materials

MDPI

Article

The Structure–Property Relationship of Pyrrolidinium and Piperidinium-Based Bromide Organic Materials

Claudio Ferdeghini [1], Andrea Mezzetta [1], Felicia D'Andrea [1], Christian Silvio Pomelli [1], Lorenzo Guazzelli [1] and Luca Guglielmero [1,2,*]

[1] Department of Pharmacy, University of Pisa, Via Bonanno 33, 56126 Pisa, Italy
[2] Scuola Normale Superiore, Piazza dei Cavalieri 7, 56126 Pisa, Italy
* Correspondence: luca.guglielmero@sns.it

Abstract: Two couples of dicationic ionic liquids, featuring pyrrolidinium and piperidinium cations and different linker chains, were prepared and characterized. 1,1′-(propane-1,3-diyl)bis(1-methylpyrrolidinium) bromide, 1,1′-(octane-1,8-diyl)bis(1-methylpyrrolidinium) bromide, 1,1′-(propane-1,3-diyl)bis (1-methylpiperidinium) bromide, and 1,1′-(octane-1,8-diyl)bis(1-methylpiperidinium) bromide were synthesized in quantitative yields and high purity and thermally characterized through TGA and DSC analysis. In this study, we propose a preliminary comparative evaluation of the effect of the linker chain length and of the size of the aliphatic ammonium ring on the thermal and solubility properties of bromide dicationic ionic liquids.

Keywords: ionic liquids (ILs); dicationic ionic liquids (DILs); thermogravimetric analysis (TGA)

Citation: Ferdeghini, C.; Mezzetta, A.; D'Andrea, F.; Pomelli, C.S.; Guazzelli, L.; Guglielmero, L. The Structure–Property Relationship of Pyrrolidinium and Piperidinium-Based Bromide Organic Materials. *Materials* **2022**, *15*, 8483. https://doi.org/10.3390/ma15238483

Academic Editor: Grzegorz Mlostoń

Received: 18 October 2022
Accepted: 23 November 2022
Published: 28 November 2022

1. Introduction

Ionic liquids (ILs) are a class of low melting organic salts, which have attracted a great amount of research interest in the past two decades [1]. Due to their peculiar physicochemical properties, including negligible vapor pressure, good thermal stability, high ionic and thermal conductivity, low flammability, wide electrochemical window, and unique solvent properties [2–8], ILs have found broad use as catalysts and as unconventional solvents for synthesis [9–12], as well as for a wide variety of different applications, spanning from electrochemical applications [13–17], biomass processing [18–20], preparation of carbon materials [21], and CO_2 capture [22], to drug delivery and utilization as potential drug components [23–25].

The great variety of different anions and cations, together with the possibility to functionalize their structure for particular applications, makes ILs versatile and flexible systems. Specific structures can be designed to suit the requirements for a specific application. The introduction of dicationic structures [26], with two positively charged groups connected by a linker chain, further expands the tunability potential of the physicochemical properties, by acting on the length of the linker chain as well as on possible asymmetries on the structure. Task specific dicationic ionic liquids (DILs) have been designed and proposed for several applications, where superior thermal stability, higher electrochemical windows, higher densities or larger surface tensions are required [26–30]. DILs have been successfully used in CO_2 capture [31], tribology [32], catalysis in organic reactions [33], zeolites preparation [34], agriculture [35], and electrochemical application [35].

The operational window for DILs is typically between the melting and degradation temperatures. Indeed, due to their very low vapor pressure they degrade before boiling. Unfortunately, the data reported in the literature are scattered, and the measuring conditions are often different. This latter issue renders a comparison of the operating ranges of DILs difficult and sometimes impossible.

In this context, we report the preparation of two couples of dicationic systems, featuring pyrrolidinium and piperidinium cations and different linker chains. The prepared

compounds were characterized by ^{1}H-NMR, ^{13}C-NMR, ATR-FTIR, and mass spectroscopy. The relationship between the structural features of the prepared salts and their physicochemical properties was investigated. The effect of the linker chain length and of the type of cationic heads on the solubility of the tested salts in a panel of commonly used solvents was determined. Finally, the thermal properties of all the prepared dicationic systems were studied through differential scanning calorimetry and thermogravimetric analysis, providing a preliminary comparative investigation on the effect of both the length of the linker chain and the size of the aliphatic ammonium ring on the thermal behavior and stability of this set of compounds.

2. Results

The desired compounds 1,1′-(propane-1,3-diyl)bis(1-methylpyrrolidinium) bromide, (**1**, [C_3Mpyrr$_2$]2Br), 1,1′-(propane-1,3-diyl)bis(1-methylpiperidinium) bromide (**2**, [C_3Mpip$_2$]2Br), 1,1′-(octane-1,3-diyl)bis(1-methylpyrrolidinium) bromide (**3**, [C_8Mpyrr$_2$]2Br), and 1,1′-(octane-1,3-diyl)bis(1-methylpiperidinium) bromide (**4**, [C_8Mpip$_2$]2Br) were prepared according to the synthetic procedure reported below (Scheme 1).

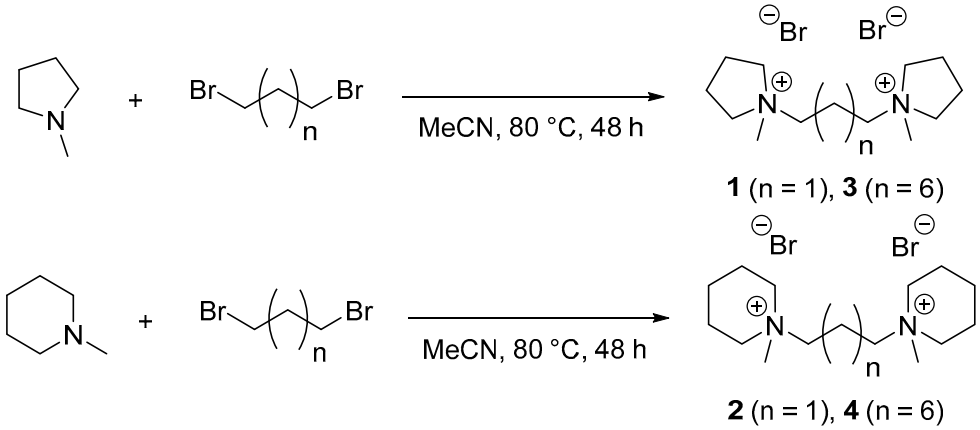

Scheme 1. Synthetic procedure adopted for the preparation of DILs **1**–**4**.

The desired compounds were obtained in a one-step reaction, adopting reaction conditions similar to the ones reported in a previous work of our research group [36]. *N*-methylpyrrolidine and *N*-methylpiperidine were used as nucleophiles for the Menshutkin reaction alternatively with 1,3-dibromopropane and 1,8-dibromooctane, in order to obtain two sets of DILs with different linker chains. The four reactions were conducted in CH_3CN at 80 °C for 48 h, obtaining the DILs as white solids in good to quantitative yields. The excess of unreacted precursors was removed by washing the solids with diethyl ether. The remaining traces of the washing solvent were finally removed under vacuum at 80 °C for 2 h. No further purification processes were needed.

^{1}H-NMR, ^{13}C-NMR, DEPT-135 NMR, and ESI-MS experiments confirmed the structures and the purities of compounds **1**–**4** (Figures S1–S12 and S21–S24, see supporting information). DEPT-135 NMR spectra (Figures S3, S6, S9, S11, see supporting information) were performed to detect the signal of the methyl group, otherwise covered by the solvent residual signal of CD_3OD in the ^{13}C-NMR (Figures S2, S5, S8, S12, see supporting information) of compounds **1**–**4**. The solubility of the prepared DILs was evaluated in a panel of solvents (Table 1). From the obtained results, there emerged a strong dependence of the solubility characteristics from the compound structure. Pyrrolidinium-based salts (**1** and **3**) displayed a higher solubility in methanol, ethanol, 2-propanol, and acetonitrile, compared to the related piperidinium salts, with the strongest difference between compounds **1** and **2**. [C_3Mpyrr$_2$]2Br (**1**) exhibited an extremely high solubility in methanol (2.526 M) and ethanol (1.470 M), while [C_3Mpip$_2$]2Br (**2**) displayed solubility values less than one fourth in methanol and even below the detectable solubility of the test for 2-propanol and acetonitrile. From the comparison between the solubility values obtained for [C_3Mpyrr$_2$]2Br (**1**)

and [C_8Mpyrr$_2$]2Br (**3**), the elongation of the linker chain provided a general reduction in the solubility in all the tested organic solvents, reducing by about half the values observed for compound **1**. On the other hand, passing from a C_3 to a C_8 linker chain for the piperidinium based systems led to an increase in the solubility, which was found to still be lower for **4** than its pyrrolidinium counterpart **3** but much higher than compound **2** for ethanol, 2-propanol, and acetonitrile. The other tested organic solvents, acetone, ethyl acetate, and dichloromethane were found to be unsuitable for the dissolution of all the tested compounds. On the other end of the scale, all the presented salts displayed an extremely high solubility in water, where only few drops of this solvent were sufficient to fully dissolve the whole sample. In these cases, it was not possible to achieve a precise determination of the solubility since no biphasic systems were obtainable, and the smallest amount of water was already enough to turn the samples into a glassy gluey body. The excellent water solubility observed for the considered salts as well as their insolubility in apolar organic solvents is consistent with the data reported by Anderson et al. for compound **1** [26,37].

Table 1. Solubility at room temperature of **1**–**4** in water (H_2O), methanol (MeOH), ethanol (EtOH), 2-propanol (iPrOH), acetonitrile (CH_3CN), acetone ($(CH_3)_2CO$), ethyl acetate (EtOAc), and dichloromethane (CH_2Cl_2).

DILs	H_2O	MeOH	EtOH	iPrOH	CH_3CN	$(CH_3)_2CO$	EtOAc	CH_2Cl_2
[C_3Mpyrr$_2$]2Br (**1**)	>2.5	2.526	1.470	0.309	0.0387	<0.003	<0.003	<0.003
[C_3Mpip$_2$]2Br (**2**)	>2.5	0.678	0.060	<0.003	<0.003	<0.003	<0.003	<0.003
[C_8Mpyrr$_2$]2Br (**3**)	>2.5	1.180	0.627	0.017	0.0134	<0.002	<0.002	<0.002
[C_8Mpip$_2$]2Br (**4**)	>2.5	0.852	0.263	0.013	0.0086	<0.002	<0.002	<0.002

The extremely sharp differences in solubility due to the small structural differences existing between the tested compounds, seen in these solubility tests, represents an interesting result for the study of the structure–property relationship of this class of dicationic systems.

The thermal behavior of [C_3Mpyrr$_2$]2Br (**1**), [C_3Mpip$_2$]2Br (**2**), [C_8Mpyrr$_2$]2Br (**3**), and [C_8Mpip$_2$]2Br (**4**) was investigated through thermal gravimetric analysis (TGA) and differential scanning calorimetry (DSC). The thermal stability was assessed by TGA, heating from 40 to 700 °C with a heating rate of 10 °C min^{-1} under a nitrogen atmosphere using a platinum crucible. The T_{peak}, T_{onset}, and $T_{start\ 5\%}$ temperatures obtained from the thermograms (Figures S13–S16, see supporting information) are reported in Table 2.

From the data reported in Table 2, no clear effects on the thermal stability of the tested compounds were appreciable for both the linker chain length and the type of cationic group. For the $T_{start\ 5\%}$ values, a not intense but still visible difference in thermal stability was appreciated between the short linker chains DILs and the long linker chain ones, with the latter starting their decomposition at slightly higher temperatures. On the other hand, the T_{onset} and T_{peak} values did not confirm this trend and appeared substantially independent from the structural parameters studied in this test. The obtained results are coherent with the ones reported in the literature for similar morpholine-based DILs bromide [30], where minimum differences were observed for the degradation temperatures of DILs with same cationic heads (Figure 1). Higher T_{peak}s were recorded for the tested pyrrolidinium and piperidinium compounds **1**–**4** with respect to the similar dicationic morpholinium systems reported by our research group in a previous work [30], showing that these cationic heads can provide more thermally stable DILs, with values almost matching those reported in the literature for imidazolium DILs [36]. More interesting differences were displayed on the thermal degradation profiles. From the dweight/dT plots of [C_3Mpip$_2$]2Br (**2**), the degradation process, even if basically occurring in a single step, was still distinct into two almost coincident separated degradations (Figure 1, Figure S14, see supporting information), Differently, this feature was not appreciable in the dweight/dT plots of [C_8Mpip$_2$]2Br (**4**), where the two main processes were so close in temperature as to be undistinguishable (Figure 1, Figure S16, see supporting information). The observed behavior was consistent with the degradation mechanism described for the

related morpholinium DILs bromide [30], even though in the present case, the double step degradation appeared much less pronounced.

Table 2. The $T_{start\ 5\%}$, T_{onset}, and T_{peak} of compounds **1**–**4**. $T_{start5\%}$ is defined as the temperature at which the weight loss of the sample is equal to 5% of the initial mass, T_{onset} is defined as temperature at the onset of the weight (%) vs. Temperature curve, and T_{peak} is defined as the temperature of the highest peak in the dweight/dT plot.

	Compound	**1**	**2**	**3**	**4**
	DIL	**[C_3Mpyrr$_2$]2Br**	**[C_3Mpip$_2$]2Br**	**[C_8Mpyrr$_2$]2Br**	**[C_8Mpip$_2$]2Br**
TGA	$T_{start\ 5\%}$ (°C)	272.8	272.3	280.3	279.8
	T_{onset} (°C)	271.2	286.4	287.9	285.9
	T_{peak} (°C)	304.7	302.9	308.6	304.6
DSC	T_m (°C)	209.2	-	174.3	-
	$\Delta_m H$(kJ/mol)	7.35		22.08	
	T_c (°C)	-	-	-	-
	$\Delta_c H$(kJ/mol)				
	$T_{s\text{-}s\ (heating)}$ (°C)	30.7	-	-	141.4
	$\Delta_{s\text{-}s(h)} H$(kJ/mol)	1.07			3.00
	$T_{s\text{-}s\ (cooling)}$ (°C)	34.2	-	-	135.8
	$\Delta_{s\text{-}s(c)} H$(kJ/mol)	1.18			3.08

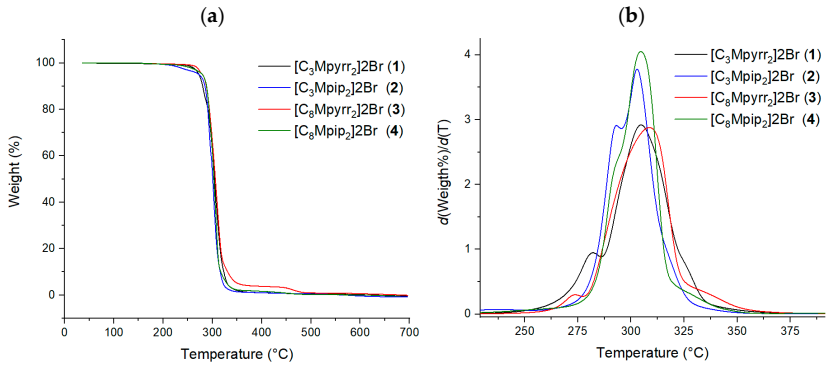

Figure 1. TGA thermograms (**a**) and derivative curves (**b**) of compounds **1**–**4** (heating ramp 10 °C min^{-1}).

Differential scanning calorimetry (DSC) analysis of compounds **1**–**4** was also performed (Figure 2), and the obtained data are reported in Table 2. Compound **1** displayed a solid–solid transition during the cooling run subsequent to the preliminary drying step (endothermic peak at 34.2 °C, 1.18 kJ mol^{-1}) and a corresponding solid–solid transition during the next heating run, characterized by both similar temperature and enthalpy (exothermic peak at 30.7 °C, 1.07 kJ mol^{-1}) (Figure 2a). A second thermal phenomenon was observed during the same heating run at 209.2 °C, identified as a melting transition. No crystallization was observed during the subsequent cooling run, and no solid–solid or melting transitions were detected in the next steps of the DSC analysis. The obtained results were in contrast to the ones reported in the literature by Anderson et al. relative to the same compound, where a low melting point was reported [26]. The melting point measure during this work was instead found to be about 30 °C higher than the one measured for the related long-chained compound **3**, which was consistent with the general melting point trend reported in the literature for different dicationic systems in relation to the length of their linker chain [26,36,38]. The different results could be due to the different water contents of the samples. For compound **2**, no thermal transition was detectable up to 260 °C, where only a small exothermic signal associated with the beginning of the thermal degradation ($T_{start\ 5\%}$ 272.3 °C) was observed (Figure S18, see supporting information). Compound **3**, sharing with **1** the presence of pyrrolidinium cationic groups, displayed a melting transition at 174.3 °C while, similar to the related compound **1**, no crystallization

was observed during the subsequent cooling step (Figure 2b). As already observed for the C_3 linker chain piperidinium salt, $[C_8Mpip_2]2Br$ (**4**) was found to not undergo any melting process up to 260 °C (Figure S20). On the other hand, solid–solid transitions were detected both during the first and the second heating–cooling cycle with an exothermic phenomenon during the 1st heating run at 141.4 °C (3.00 KJ mol^{-1}) and a related endothermic one during the 1st cooling run at 135.8 °C (3.08 KJ mol^{-1}) (Figure 2c). Only minimum differences in terms of temperature and associated enthalpy were appreciable between the two cycles at 10 °C min^{-1}, and the same peak temperatures were also found for a supplemental cycle performed at 5 °C min^{-1} (Figures S20 and S21, see supporting information). The identification of these peaks as solid–solid transitions was confirmed by the use of the Kofler technique, which clearly showed no melting transitions up to above 200 °C (Figure S30, see supporting information).

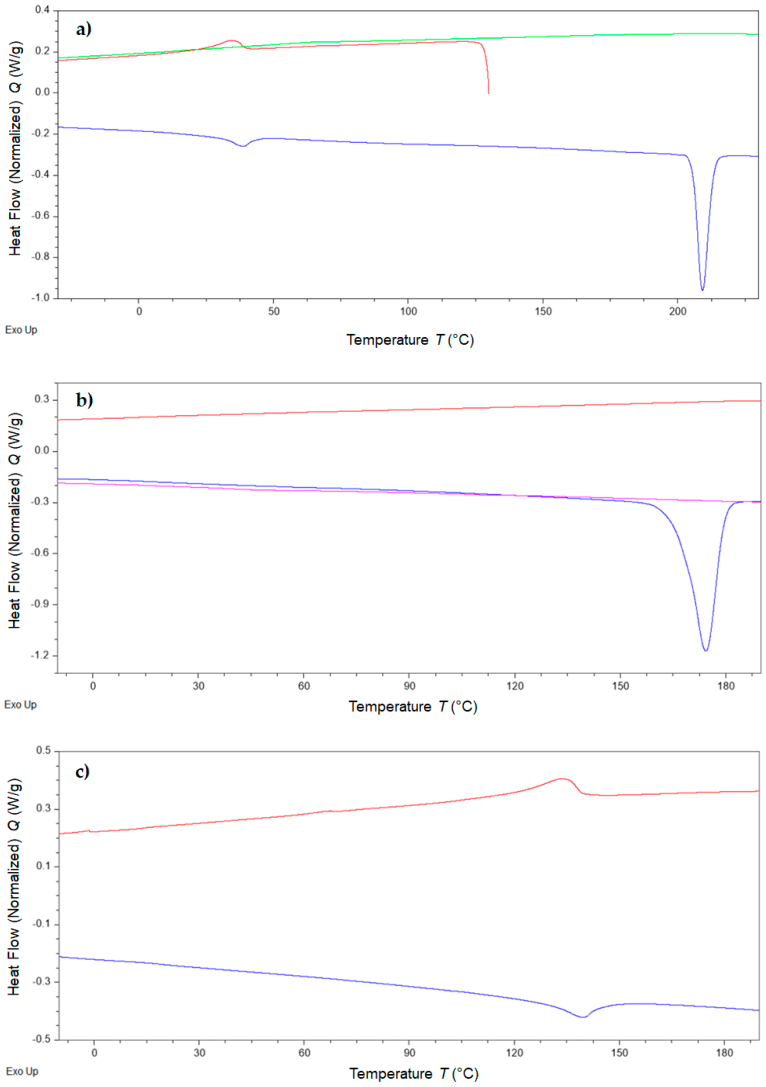

Figure 2. (**a**) DSC thermograms of $[C_8Mpyrr_2]2Br$ (**1**), red: cooling ramp after initial drying step (10 °C min^{-1}), blue: 1st heating ramp (10 °C min^{-1}), green: 1st cooling ramp (10 °C min^{-1}); (**b**) DSC thermograms of $[C_8Mpyrr_2]2Br$ (**3**), blue: 1st heating ramp (10 °C min^{-1}), red: 1st cooling ramp (10 °C min^{-1}), purple: 2nd heating ramp (10 °C min^{-1}); (**c**) DSC thermograms of $[C_8Mpip_2]2Br$ (**4**), blue: 1st heating ramp (10 °C min^{-1}), red: 1st cooling ramp (10 °C min^{-1}).

For ILs, the operative range defines the interval of temperatures where the studied system is liquid and usable for applications. It is usually determined by considering the degradation temperature obtained from the TGA as the upper utilization limit and the

melting point measured by DSC as the lowest limit. Even though not classifiable as an ionic liquid with full rights due to its high melting point, an operative range of 106.0 °C was indicated for compound **3** (considering the upper limit as the $T_{start\ 5\%}$ value). It is important to notice that for a meaningful comparison of operative ranges of different systems, thermal analyses need to have the same experimental settings. In conclusion, both the length of the linker chain and the type of cation heads represented an influential element in the determination of the thermal behavior of the considered salts, with the pyrrolidinium C_8 linker compounds melting at a sensibly higher temperature with respect to the solid–solid transition observed for its related piperidinium compound, and the C_3 systems, on the other hand, not manifesting any detectable thermal transition.

3. Materials and Methods

3.1. General Information

NMR spectra were recorded with a Bruker Avance II (Bruker Italia S.r.l., Milano, Italy) operating at 400 (^{1}H) and 100 MHz (^{13}C). The first-order proton chemical shifts were referenced to the residual CD_3OD (δ_H 3.31, δ_C 49.03). The chemical shifts were given in δ. The following abbreviations were used; s = singlet, m = multiplet.

ATR-FTIR spectra were recorded with an IR Cary 600 FTIR spectrometer (Agilent Technologies, Santa Clara, CA, USA) using a macroATR accessory with a diamond crystal. The spectra were measured in a range from 4000 to 500 cm^{-1}, with 32 scans both for background and samples.

High resolution mass spectra were acquired on an Orbitrap Q Exactive Plus with H-ESI source (Thermo Fischer Scientific Inc., Bremen, Germany) in ESI positive ionization mode operating with the following parameters: a spray voltage of 3400 V, capillary temperature of 290 °C, S-lens RF level 50, sheat gas (N_2) 24 arbitrary unit, and auxiliary gas (N_2) 5 arbitrary unit. The data were elaborated with Xcalibur software.

All reagents and solvents were obtained from Merck Life Science S.r.l. (Darmstadt, Germany) or Thermo Fisher (Germany) and used without further purification.

The thermal stability of the synthesized ILs was investigated by thermal gravimetric analysis (TGA), using a TA Instruments Q500 TGA (TA Instruments, New Castle, DE, USA). The temperature calibration was performed using a nickel standard, and for weight calibration, we used weight standards (1 g, 500 mg, and 100 mg). All standards were supplied by TA Instruments Inc. The ILs (5–15 mg) were heated in a platinum crucible as a sample holder from 40 °C to 700 °C at 10 °C/min under nitrogen (90 mL/min). The TGA experiments were carried out in triplicate.

The thermal behavior of the ionic liquids was analyzed by a differential scanning calorimeter TA Instruments DSC, Q250 (TA Instruments, New Castle, DE, USA). Dry high-purity N_2 gas with a flow rate of 30 mL/min was purged through the sample. The sample (2–5 mg) was loaded in hermetic aluminum crucibles and dried at 130 °C for 30 min. Then, the phase behavior was explored under nitrogen atmosphere in the temperature range of −90 to 260 °C, depending on the analyzed compound. The enthalpy was also calibrated using indium (melting enthalpy $\Delta_m H$ = 28.71 J/g). The DSC experiments were carried out in duplicate.

The solubility of compounds **1–4** in a panel of selected solvents was determined by a gravimetric approach, at room temperature. To the selected compound a quantity of solvent was added, enough to retain some solid residue, in order to obtain a saturated solution. The mixture was stirred for 10 min at reflux temperature and then for 2 h in a bath at 25 °C. If the solid was found to be completely solubilized, more salt was added, and the dissolution procedure was repeated. A carefully measured volume of the decanted solution was taken and dried under vacuum for 2 h at 80 °C. The ratio between the obtained mass and the taken volume was used to calculate the concentration of the selected compound in the solvent at the saturation point.

3.2. General Procedure for the Synthesis of Compounds **1**–**4**

Compounds **1**–**4** were obtained following a general procedure previously reported by our group [36]. In a flask, to a solution of 2.1 equiv (15 mmol) of *N*-methyl heterocycle in 5 mL of CH_3CN, a solution of 1 equiv of 1,n-dibromoalkane in 15 mL of CH_3CN was added dropwise. The reaction mixture was then heated and stirred at 80 °C for 48 h. The solvent was removed under reduced pressure, and the obtained solid was washed with Et_2O (3 × 50 mL); then, it was dried under reduced pressure affording the desired product in quantitative yield as a white solid.

3.2.1. Synthesis of Ionic Liquid 1 [C_3Mpyrr_2]2Br

The preparation of **1** (97% yield, hygroscopic white solid) was performed according to the general procedure. ^{1}H-NMR (CD_3OD) δ: 3.66 (m, 8H, 4 × N$CH_2$$CH_2$ pyrrolidinium), 3.52 (m, 4H, 2 × N$CH_2$$CH_2$ linker chain), 3.20 (s, 6H, 2 × NCH_3), 2.43 (m, 2H, $NCH_2CH_2CH_2N$), and 2.28 (m, 8H, NCH_2CH_2 pyrrolidinium). The obtained spectrum was in agreement with the literature data [26]. Minor variations in the chemical shift were ascribable to the different deuterated solvent used. ^{13}C-NMR (CD_3OD) δ: 66.0 (N$CH_2$$CH_2$ pyrrolidinium), 61.5 (N$CH_2$$CH_2$ linker chain), 49.5 (NCH_3), 22.7 (NCH_2CH_2 pyrrolidinium), and 20.7 ($NCH_2CH_2CH_2N$ linker chain). ATR-FTIR (cm^{-1}): 3001, 2959, 2888, 1456, 1420, 1373, 1306, 1054, 999, 930, 911, 827, and 763. ESI-MS positive mode calculated for $[C_{13}H_{28}N_2]^{2+}$: m/z = 106.1121 (z = 2); found: m/z = 106.1126 (z = 2).

3.2.2. Synthesis of Ionic Liquid 2 [C_3Mpip_2]2Br

The preparation of **2** (86% yield, hygroscopic white solid) was performed according to the general procedure. ^{1}H-NMR (CD_3OD) δ: 3.54 (m, 12H, 6 × N$CH_2$$CH_2$ piperidinium and linker chain), 3.21 (s, 6H, 2 × NCH_3), 2.36 (m, 2H, $NCH_2CH_2CH_2N$ linker chain), 1.97 (m, 8H, 4 × NCH_2CH_2 piperidinium), and 1.73 (m, 4H, 2 × $NCH_2CH_2CH_2$ piperidinium). ^{13}C-NMR (CD_3OD) δ: 62.8 (N$CH_2$$CH_2$ piperidinium), 60.9 (N$CH_2$$CH_2$ linker chain), 50.0 (NCH_3), 22.0 ($NCH_2CH_2CH_2$ piperidinium), 21.0 (NCH_2CH_2 piperidinium), and 17.1 ($NCH_2CH_2CH_2N$ linker chain). ATR-FTIR (cm^{-1}): 2997, 2966, 2946, 2903, 2858, 1490, 1468, 1445, 1403, 1349, 1329, 1278, 1234, 1196, 1112, 1058, 1037, 996, 970, 944, 912, 889, 867, 825, 795, and 755. ESI-MS positive mode calculated for $[C_{15}H_{32}N_2]^{2+}$: m/z = 120.1277 (z = 2); found: m/z = 120.1278 (z = 2).

3.2.3. Synthesis of Ionic Liquid 3 [C_8Mpyrr_2]2Br

The preparation of **3** (99% yield, hygroscopic white solid) was performed according to the general procedure. ^{1}H-NMR (CD_3OD) δ: 3.58 (m, 8H, 4 × N$CH_2$$CH_2$ pyrrolidinium), 3.43 (m, 4H, 2 × N$CH_2$$CH_2$ linker chain), 3.11 (s, 6H, 2 × NCH_3), 2.24 (m, 8H, 4 × NCH_2CH_2 pyrrolidinium), 1.84 (m, 4H, 2 × NCH_2CH_2 linker chain), and 1.46 (m, 8H, 2 × $NCH_2CH_2CH_2$ and 2 × $NCH_2CH_2CH_2CH_2$ linker chain). ^{13}C-NMR (CD_3OD) δ: 65.5 (N$CH_2$$CH_2$ linker chain), 65.4 (N$CH_2$$CH_2$ pyrrolidinium), 48.9 (NCH_3), 29.7 ($NCH_2CH_2CH_2CH_2$ linker chain), 27.2 ($NCH_2CH_2CH_2$ linker chain), 24.7 (NCH_2CH_2 linker chain), and 22.6 (NCH_2CH_2 pyrrolidinium). ATR-FTIR (cm^{-1}): 3008, 2937, 2856, 1473, 1455, 1413, 1310, 1049, 1000, 956, 930, 837, and 729. ESI-MS positive mode calculated for $[C_{18}H_{38}N_2]^{2+}$: m/z = 141.1512 (z = 2); found: m/z = 141.1514 (z = 2).

3.2.4. Synthesis of Ionic Liquid 4 [C_8Mpip_2]2Br

The preparation of **4** (97% yield, hygroscopic white solid) was performed according to the general procedure. ^{1}H-NMR (CD_3OD) δ: 3.42 (m, 12H, 6 × N$CH_2$$CH_2$ piperidinium and linker chain), 3.10 (s, 6H, 2 × NCH_3), 1.92 (m, 8H, 4 × NCH_2CH_2 piperidinium), 1.60–1.85 (m, 8H, 4 × NCH_2CH_2 linker chain and 4 × $NCH_2CH_2CH_2$ piperidinium), and 1.46 (m, 8H 4 × $NCH_2CH_2CH_2$ and 4 × $NCH_2CH_2CH_2CH_2$ linker chain). ^{13}C-NMR (CD_3OD) δ: 65.1 (N$CH_2$$CH_2$ piperidinium), 62.2 (N$CH_2$$CH_2$ linker chain), 48.2 (NCH_3), 29.8 ($NCH_2CH_2CH_2CH_2$ linker chain), 27.2 ($NCH_2CH_2CH_2$ linker chain), 22.7 (NCH_2CH_2 linker chain), 22.1 ($NCH_2CH_2CH_2$ piperidinium), and 21.0 (NCH_2CH_2 piperidinium). ATR-

FTIR (cm^{-1}): 2927, 2876, 2853, 1477, 1460, 1447, 1401, 1329, 1273, 1235, 1200, 1080, 1033, 983, 946, 911, 884, 865, 729, and 606. ESI-MS positive mode calculated for $[C_{20}H_{42}N_2]^{2+}$: m/z = 155.1669 (z = 2); found: m/z = 155.1670 (z = 2).

4. Conclusions

In conclusion, four bromide dicationic organic salts were synthesized in high purity and quantitative yields. All the compounds were characterized through ESI-MS, ^{1}H-NMR, ^{13}C-NMR, DEPT-135 NMR, and ATR-FTIR, their solubility was measured in a panel of commonly used solvents, and their operative range was investigated by TGA and DSC techniques. The thermogravimetric analysis showed a good thermal stability both for pyrrolidinium and piperidinium salts, comparable to the one exhibited by imidazolium DILs, and a substantial independence of the thermal stability from the linker chain. The thermal behavior was, on the other hand found, to be sharply influenced by the structure of the studied compounds. The pyrrolidinium salts displayed high melting temperatures, while the piperidinium compounds were found to degrade before the melting point. The effect of the linker chain was also appreciable with a lower melting point reported for the dicationic system with a longer linker chain, coherent with the behavior manifested by other classes of dicationic ionic liquids. As a result of this study, the investigated compounds should more correctly be referred to as dicationic organic salts, due to their high melting temperatures. Nevertheless, the use of compounds **1**–**4** as precursors for the preparation of salts featuring the same dicationic structure but different anions can predictably lead to the formation of proper dicationic ionic liquid systems. Moreover, the solubility study evidenced a remarkable difference between the related pyrrolidinium and piperidinium dicationic salts, with the latter being less soluble in the whole panel of tested solvents. This characteristic appears to be amplified by the short linker chains, with compounds **1** and **2** respectively displaying the highest and the lowest observed solubility for each solvent.

The results obtained in this study provided some interesting insights on the presence of a strong relationship between the structural and physicochemical properties in pyrrolidinium and piperidinium-based dicationic systems.

Supplementary Materials: The following supporting information can be downloaded at: https://www.mdpi.com/article/10.3390/ma15238483/s1, Figures S1–S12: ^{1}H-NMR, ^{13}C-NMR, and DEPT-135 NMR spectra of compounds **1**–**4**; Figures S13–S16: TGA profiles of compounds **1**–**4**; Figures S16–S21: DSC thermograms of compounds **1**–**4**, Figures S22–S25: ESI-MS spectra of compounds **1**–**4**, Figures S26–S29: ATR-FTIR spectra of compounds **1**–**4**, Figure S30: pictures from the determination of the melting point of compound **1** through the Kofler technique.

Author Contributions: Conceptualization, A.M. and L.G. (Luca Guglielmero); methodology, L.G. (Lorenzo Guazzelli) and C.S.P.; synthesis, C.F.; NMR characterization, C.F. and L.G. (Luca Guglielmero); thermal analysis, C.F.; data curation, L.G. (Luca Guglielmero), A.M. and F.D.A; writing—original draft preparation, L.G. (Luca Guglielmero) and A.M.; writing—review and editing, L.G. (Lorenzo Guazzelli), F.D., and C.S.P.; supervision, L.G. (Lorenzo Guazzelli) and C.S.P. All authors have read and agreed to the published version of the manuscript.

Funding: This work is supported by the Università di Pisa under the "PRA-Progetti di Ricerca di Ateneo" (Institutional Research Grants, PRA_2020–2021)—Project no PRA_2020_58—Agenti innovativi e nanosistemi per target molecolari nell'ambito dell'oncologia di precisione.

Institutional Review Board Statement: Not applicable.

Informed Consent Statement: Not applicable.

Data Availability Statement: Not applicable.

Conflicts of Interest: The authors declare no conflict of interest.

References

1. Singh, S.K.; Savoy, A.W. Ionic Liquids Synthesis and Applications: An Overview. *J. Mol. Liq.* **2020**, *297*, 112038. [CrossRef]

2. Piatti, E.; Guglielmero, L.; Tofani, G.; Mezzetta, A.; Guazzelli, L.; D'Andrea, F.; Roddaro, S.; Pomelli, C.S. Ionic Liquids for Electrochemical Applications: Correlation between Molecular Structure and Electrochemical Stability Window. *J. Mol. Liq.* **2022**, *364*, 120001. [CrossRef]
3. Tokuda, H.; Hayamizu, K.; Ishii, K.; Susan, M.A.B.H.; Watanabe, M. Physicochemical Properties and Structures of Room Temperature Ionic Liquids. 2. Variation of Alkyl Chain Length in Imidazolium Cation. *J. Phys. Chem. B* **2005**, *109*, 6103–6110. [CrossRef] [PubMed]
4. Chen, Q.-L.; Wu, K.-J.; He, C.-H. Thermal Conductivity of Ionic Liquids at Atmospheric Pressure: Database, Analysis, and Prediction Using a Topological Index Method. *Ind. Eng. Chem. Res.* **2014**, *53*, 7224–7232. [CrossRef]
5. Zech, O.; Stoppa, A.; Buchner, R.; Kunz, W. The Conductivity of Imidazolium-Based Ionic Liquids from (248 to 468) K. B. Variation of the Anion. *J. Chem. Eng. Data* **2010**, *55*, 1774–1778. [CrossRef]
6. Xue, Z.; Qin, L.; Jiang, J.; Mu, T.; Gao, G. Thermal, Electrochemical and Radiolytic Stabilities of Ionic Liquids. *Phys. Chem. Chem. Phys.* **2018**, *20*, 8382–8402. [CrossRef]
7. Xu, C.; Cheng, Z. Thermal Stability of Ionic Liquids: Current Status and Prospects for Future Development. *Processes* **2021**, *9*, 337. [CrossRef]
8. Barulli, L.; Mezzetta, A.; Brunetti, B.; Guazzelli, L.; Vecchio Ciprioti, S.; Ciccioli, A. Evaporation Thermodynamics of the Tetraoctylphosphonium Bis(Trifluoromethansulfonyl)Imide([P_{8888}]NTf_2) and Tetraoctylphosphonium Nonafluorobutane-1-Sulfonate ([P_{8888}]NFBS) Ionic Liquids. *J. Mol. Liq.* **2021**, *333*, 115892. [CrossRef]
9. Hallett, J.P.; Welton, T. Room-Temperature Ionic Liquids: Solvents for Synthesis and Catalysis. 2. *Chem. Rev.* **2011**, *111*, 3508–3576. [CrossRef]
10. Radai, Z.; Kiss, N.Z.; Keglevich, G. An Overview of the Applications of Ionic Liquids as Catalysts and Additives in Organic Chemical Reactions. *Curr. Org. Chem.* **2018**, *22*, 533–556. [CrossRef]
11. Zhang, Q.; Zhang, S.; Deng, Y. Recent Advances in Ionic Liquid Catalysis. *Green Chem.* **2011**, *13*, 2619. [CrossRef]
12. Javaherian, M.; Saghanezhad, S.J. Synthesis, Characterization and Applications of Dicationic Ionic Liquids in Organic Synthesis. *Mini Rev. Org. Chem.* **2020**, *17*, 450–464. [CrossRef]
13. Guglielmero, L.; Langroudi, M.M.; Al Khatib, M.; de Oliveira, M.A.C.; Mecheri, B.; de Leo, M.; Mezzetta, A.; Guazzelli, L.; Giglioli, R.; Epifanio, A.D.; et al. Electrochemical and Spectroscopic Study of Vanadyl Acetylacetonate–Ionic Liquids Interactions. *Electrochim. Acta* **2021**, *373*, 137865. [CrossRef]
14. Guglielmero, L.; Mero, A.; Mezzetta, A.; Tofani, G.; D'Andrea, F.; Pomelli, C.S.; Guazzelli, L. Novel Access to Ionic Liquids Based on Trivalent Metal–EDTA Complexes and Their Thermal and Electrochemical Characterization. *J. Mol. Liq.* **2021**, *340*, 117210. [CrossRef]
15. Watanabe, M.; Thomas, M.L.; Zhang, S.; Ueno, K.; Yasuda, T.; Dokko, K. Application of Ionic Liquids to Energy Storage and Conversion Materials and Devices. *Chem. Rev.* **2017**, *117*, 7190–7239. [CrossRef] [PubMed]
16. Bahadori, L.; Boyd, R.; Warrington, A.; Shafeeyan, M.S.; Nockemann, P. Evaluation of Ionic Liquids as Electrolytes for Vanadium Redox Flow Batteries. *J. Mol. Liq.* **2020**, *317*, 114017. [CrossRef]
17. Jónsson, E. Ionic Liquids as Electrolytes for Energy Storage Applications—A Modelling Perspective. *Energy Storage Mater.* **2020**, *25*, 827–835. [CrossRef]
18. Isik, M.; Sardon, H.; Mecerreyes, D. Ionic Liquids and Cellulose: Dissolution, Chemical Modification and Preparation of New Cellulosic Materials. *Int. J. Mol. Sci.* **2014**, *15*, 11922–11940. [CrossRef]
19. Berga, L.; Bruce, I.; Nicol, T.W.J.; Holding, A.J.; Isobe, N.; Shimizu, S.; Walker, A.J.; Reid, J.E.S.J. Cellulose Dissolution and Regeneration Using a Non-Aqueous, Non-Stoichiometric Protic Ionic Liquid System. *Cellulose* **2020**, *27*, 9593–9603. [CrossRef]
20. Husanu, E.; Mero, A.; Rivera, J.G.; Mezzetta, A.; Ruiz, J.C.; D'Andrea, F.; Pomelli, C.S.; Guazzelli, L. Exploiting Deep Eutectic Solvents and Ionic Liquids for the Valorization of Chestnut Shell Waste. *ACS Sustain. Chem. Eng.* **2020**, *8*, 18386–18399. [CrossRef]
21. Brzęczek-Szafran, A.; Gaida, B.; Blacha-Grzechnik, A.; Matuszek, K.; Chrobok, A. Bioderived Ionic Liquids and Salts with Various Cyano Anions as Precursors for Doped Carbon Materials. *Int. J. Mol. Sci.* **2021**, *22*, 10426. [CrossRef] [PubMed]
22. Soares, B.F.; Nosov, D.R.; Pires, J.M.; Tyutyunov, A.A.; Lozinskaya, E.I.; Antonov, D.Y.; Shaplov, A.S.; Marrucho, I.M. Tunning CO_2 Separation Performance of Ionic Liquids through Asymmetric Anions. *Molecules* **2022**, *27*, 413. [CrossRef] [PubMed]
23. Ali, M.K.; Moshikur, R.M.; Wakabayashi, R.; Moniruzzaman, M.; Kamiya, N.; Goto, M. Biocompatible Ionic Liquid Surfactant-Based Microemulsion as a Potential Carrier for Sparingly Soluble Drugs. *ACS Sustain. Chem. Eng.* **2020**, *8*, 6263–6272. [CrossRef]
24. Florio, W.; Becherini, S.; D'Andrea, F.; Lupetti, A.; Chiappe, C.; Guazzelli, L. Comparative Evaluation of Antimicrobial Activity of Different Types of Ionic Liquids. *Mater. Sci. Eng. C* **2019**, *104*, 109907. [CrossRef]
25. Stachowiak, W.; Wysocki, M.; Niemczak, M. "Bitter" Results: Toward Sustainable Synthesis of the Most Bitter Substances, Denatonium Saccharinate and Denatonium Benzoate, Starting from a Popular Anesthetic, Lidocaine. *J. Chem. Educ.* **2022**, *99*, 1604–1611. [CrossRef]
26. Anderson, J.L.; Ding, R.; Ellern, A.; Armstrong, D.W. Structure and Properties of High Stability Geminal Dicationic Ionic Liquids. *J. Am. Chem. Soc.* **2005**, *127*, 593–604. [CrossRef]
27. Shirota, H.; Mandai, T.; Fukazawa, H.; Kato, T. Comparison between Dicationic and Monocationic Ionic Liquids: Liquid Density, Thermal Properties, Surface Tension, and Shear Viscosity. *J. Chem. Eng. Data* **2011**, *56*, 2453–2459. [CrossRef]
28. Pitawala, J.; Matic, A.; Martinelli, A.; Jacobsson, P.; Koch, V.; Croce, F. Thermal Properties and Ionic Conductivity of Imidazolium Bis(Trifluoromethanesulfonyl)Imide Dicationic Ionic Liquids. *J. Phys. Chem. B* **2009**, *113*, 10607–10610. [CrossRef]

29. Vieira, J.C.B.; Villetti, M.A.; Frizzo, C.P. Thermal Stability and Decomposition Mechanism of Dicationic Imidazolium-Based Ionic Liquids with Carboxylate Anions. *J. Mol. Liq.* **2021**, *330*, 115618. [CrossRef]
30. Ferdeghini, C.; Guazzelli, L.; Pomelli, C.S.; Ciccioli, A.; Brunetti, B.; Mezzetta, A.; Vecchio Ciprioti, S. Synthesis, Thermal Behavior and Kinetic Study of N-Morpholinium Dicationic Ionic Liquids by Thermogravimetry. *J. Mol. Liq.* **2021**, *332*, 115662. [CrossRef]
31. Avila, J.; Lepre, L.F.; Goloviznina, K.; Guazzelli, L.; Pomelli, C.S.; Chiappe, C.; Pádua, A.; Costa Gomes, M. Improved Carbon Dioxide Absorption in Double-Charged Ionic Liquids. *Phys. Chem. Chem. Phys.* **2021**, *23*, 23130–23140. [CrossRef] [PubMed]
32. Yu, Q.; Zhang, C.; Dong, R.; Shi, Y.; Wang, Y.; Bai, Y.; Zhang, J.; Cai, M.; Zhou, F.; Liu, W. Physicochemical and Tribological Properties of Gemini-Type Halogen-Free Dicationic Ionic Liquids. *Friction* **2021**, *9*, 344–355. [CrossRef]
33. Guglielmero, L.; Mezzetta, A.; Pomelli, C.S.; Chiappe, C.; Guazzelli, L. Evaluation of the Effect of the Dicationic Ionic Liquid Structure on the Cycloaddition of CO_2 to Epoxides. *J. CO_2 Util.* **2019**, *34*, 437–445. [CrossRef]
34. Lee, S.-H.; Lee, D.-K.; Shin, C.-H.; Park, Y.-K.; Wright, P.A.; Lee, W.M.; Hong, S.B. Synthesis, Characterization, and Catalytic Properties of Zeolites IM-5 and NU-88. *J. Catal.* **2003**, *215*, 151–170. [CrossRef]
35. Pernak, J.; Niemczak, M.; Rzemieniecki, T.; Marcinkowska, K.; Praczyk, T. Dicationic Herbicidal Ionic Liquids Comprising Two Active Ingredients Exhibiting Different Modes of Action. *J. Agric. Food Chem.* **2022**, *70*, 2545–2553. [CrossRef] [PubMed]
36. Mezzetta, A.; Perillo, V.; Guazzelli, L.; Chiappe, C. Thermal Behavior Analysis as a Valuable Tool for Comparing Ionic Liquids of Different Classes. *J. Therm. Anal. Calorim.* **2019**, *138*, 3335–3345. [CrossRef]
37. Armstrong, D.; Anderson, J. High Stability Diionic Liquid Salts. U.S. Patent US 2006/0025598A1, 2 February 2006.
38. Guglielmero, L.; Mezzetta, A.; Guazzelli, L.; Pomelli, C.S.; D'Andrea, F.; Chiappe, C. Systematic Synthesis and Properties Evaluation of Dicationic Ionic Liquids, and a Glance into a Potential New Field. *Front. Chem.* **2018**, *6*, 612. [CrossRef] [PubMed]